Thermal decomposition of calcium copper acetate hexahydrate by simultaneous measurement of controlled-rate thermogravimetry and mass spectrometry (CRTG–MS)

Tadashi Arii[a,*], Yoshio Masuda[b]

[a]*Thermal Analysis Division, RIGAKU Corporation, 3-9-12 Matubara, Akishima, Tokyo 196-8666, Japan*
[b]*Department of Environmental Science, Faculty of Science, Niigata University, Ikarashi-2, Niigata 950-2181, Japan*

Abstract

The thermal decomposition of calcium copper acetate hexahydrate, $CaCu(CH_3CO_2)_4 \cdot 6H_2O$, in an inert atmosphere has been studied successfully by means of thermogravimetry (TG) or controlled-rate thermogravimetry (CRTG), both combined with simultaneous evolved gas analysis (EGA) using mass spectrometry (MS). CRTG is useful to simplify the complicated successive reactions and to study the mechanism of the thermal decomposition. The determination of the residual intermediates provides powerful information to analyze the decomposition mechanism. Compared with the conventional linear heating method the CRTG–MS method offers an invaluable interpretation for the complex process in the thermal events.

The features of the thermal decomposition observed by the conventional TG were different from those by CRTG, so that the decomposition seems to proceed through different mechanisms in TG and CRTG. The X-ray diffraction profiles of the intermediate products support this expectation. The decomposition mechanism of $CaCu(CH_3CO_2)_4 \cdot 6H_2O$ was proposed. © 1999 Elsevier Science B.V. All rights reserved.

Keywords: Controlled-rate thermogravimetry; Mass spectrometry; Simultaneous measuring apparatus; Thermal decomposition; Calcium copper acetate hexahydrate

1. Introduction

Calcium copper acetate hexahydrate, $CaCu(CH_3CO_2)_4 \cdot 6H_2O$, is known as an example of an incongruent saturating double salt. This compound is a normal paramagnetic crystal and has tetragonal prismatic crystal structure [1]. Only $CaCd(CH_3CO_2)_4 \cdot 6H_2O$ has been found to be isomorphous with $CaCu(CH_3CO_2)_4 \cdot 6H_2O$. Its structure consists of infinite acetatobridged chains of alternate metal ions that are linked together via water molecules which form 12-membered water cages [2]. Here, the two within the six water molecules coordinate only to Ca ion and the remaining water molecules are hydrogen-bonded with oxygen ions in the acetate anions coordinated to Cu ion. In view of the current interest in the relation of the stereochemistry and the thermal property including these water molecules, Masuda et al. reported that the dehydration behavior of both hydrates is influenced by the delicate difference between their crystal structures [3,4]. However,

*Corresponding author. Fax: +81-04-544-9650
E-mail address: t-arii@rigaku.co.jp (T. Arii)

the thermal decomposition following the dehydration has been scarcely reported. The decomposition behavior of these complicated coordination complexes is also particularly attractive for studying such structural physico-chemical phenomenon.

Since the thermal decomposition frequently proceeds through the various steps accompanying several intermediate formations, controlling the rate of the various steps is important to interpret the formation mechanism of intermediates. Then, these steps are strongly influenced by the conditions such as the heating rates and the atmospheres including self-generated atmosphere. From this point of view, thermal analysis with evolved gas analysis (EGA) is particularly valuable to obtain direct chemical information about volatile products in the course of decomposition process.

Recently simultaneous measuring methods combined the duplicate or triplicate techniques have been developed rapidly and their achievements have attracted much attention [5–11]. Simultaneous technique of coupling TG and Fourier transform infrared spectroscopy (FTIR) or mass spectrometry (MS), where the experimental results are displayed in three dimensions such as the temperature, the mass number and the abundance, have been developed in the past decade [7–11]. TG–MS is most effectively to identify the evolved products caused by thermal decomposition, and TG–MS measurement makes possible to determine more exactly the mechanism of decomposition process.

On the other hand, another sophisticated approach for the thermal analysis such as controlled-rate thermal analysis (CRTA) or sample controlled thermal analysis (SCTA) has been developed. In the CRTA, the rate of reaction is controlled by controlling the sample temperature [12–17]. A constant reaction rate or a constant pressure of the evolved species in the reaction environment can be easily achieved at present. In our previous papers, we demonstrated that controlled-rate thermogravimetry (CRTG) was superior to offer significant advantages than the conventional linear heating TG [18–20]. The CRTG provides not only an improved sensitivity and resolution as well as the conventional linear heating TG but also more exact kinetic data than that.

Our focus is first of all on the interpretation of the actual decomposition mechanism of calcium copper acetate hexahydrate. In the present paper, we analyze the complicated decomposition behavior of $CaCu(CH_3CO_2)_4 \cdot 6H_2O$ in more detail by the use of CRTG, TG–DTA–MS (simultaneous measurement of TG, DTA and MS) and CRTG–MS (simultaneous measurement of CRTG and MS) in helium atmosphere. Then, we demonstrate the effectiveness of these techniques, and discuss the difference of the decomposition mechanisms derived from the linear heating TG and the CRTG.

2. Experimental

2.1. Reagent

Calcium copper acetate hexahydrate of tetragonal prismatic crystals was synthesized from solutions of calcium acetate and copper acetate, and was recrystallized from distilled water. Then, it was pulverized with a mortar and pestle, and sieved to a narrow fraction of mesh size 100–150. A sample of about 30 mg was weighed into an open platinum crucible and measured in helium atmosphere.

2.2. Apparatus

The CRTA apparatus used was a Rigaku Thermo Plus TG–DTA 8120D thermogravimetry–differential thermal analyzer upgraded with a dynamic TG–DTA module, and similar apparatuses described in the previous papers [18,19]. A sequence of experiments was carried out by use of the full automated and computerized CRTG, in which the mass loss was maintained at a pre-selected value of constant rate. The sample was heated in a platinum crucible of 5 mm diameter and 2.5 mm height, in helium atmosphere (a flow rate of 300 cm^3 min^{-1}). In the CRTG experiment, the sample is heated at first at a constant heating rate of 5°C min^{-1}, and then at a proper switchover temperature 190°C (above the dehydration region) the mass loss rate is maintained at 0.06% min^{-1} by the automatic control of the heating/cooling rate mode.

The mass spectrum of the gases evolved was monitored simultaneously with a Rigaku Thermo Mass system coupled with the dynamic TG–DTA via the gas interface capillary heated at 250°C. The quadrupole mass spectrometer (QMS), Anelva model MQ-200TS

with a thoria-coated iridium filament, was operated in an electron impact mode, under the conditions of the ionization potential of 70 eV and mass region for the detection, 10–80 amu. Low background pressure of nitrogen ($m/z = 28$) and water vapor remaining in the atmosphere was achieved, so that carbon monoxide ($m/z = 28$) and water vapor evolved from the sample was successfully evaluated. The MS data were recorded simultaneously with TG and DTA curves. The mass spectrometer was used to measure the total ion current (TIC) or the mass spectrum in which the selected m/z values was measured to identify the evolved gases corresponding to the mass losses. NIST/EPA/NIH chemical and structural database was used to assign the mass spectrum of an unknown compound.

X-ray diffraction (XRD) analysis to identify the crystalline phases was performed on a Rigaku/RINT2500 X-ray diffractometer using nickel-filtered CuK$_\alpha$ radiation ($\lambda = 1.5405$ Å) and a graphite monochromator. A line shape X-ray source was operated at 50 kV and 300 mA, and the data were collected in the range of $3° < 2\theta < 90°$ with an interval of $0.02°$ and a scan speed of $4°\,min^{-1}$. The samples were quenched quickly from the TG–DTA (CRTG) apparatus at the predetermined temperature.

3. Results and discussion

Fig. 1 shows the TG, DTG and DTA curves for the thermal decomposition of CaCu(CH$_3$CO$_2$)$_4$·6H$_2$O
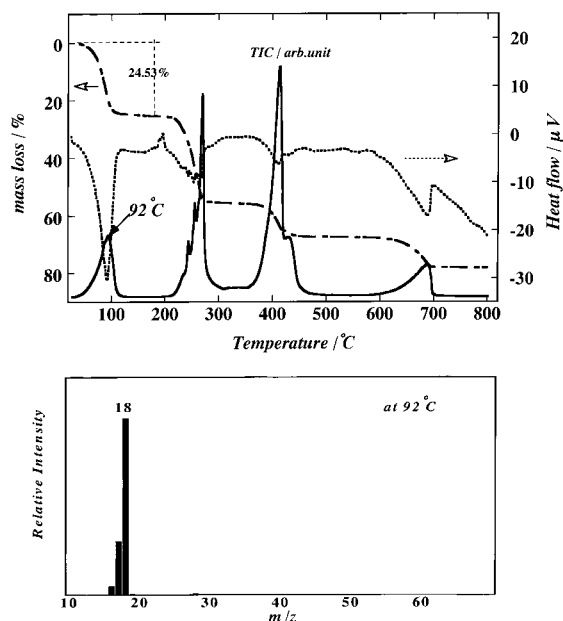

Fig. 2. Overall TG, DTG and TIC curves for simultaneous TG–DTA–MS at $3°C\,min^{-1}$ and mass spectrum observed at $92°C$ in TIC.

obtained by conventional constant heating rate of $3°C\,min^{-1}$. The thermal decomposition was roughly divided into four steps. In the first stage, the mass loss of 24.53% accompanied with a clear DTA peak at $92°C$ was recognized by use of the TG–DTA–MS (Fig. 2). The TG, DTG and DTA curves were in good correspondence with the simultaneous TIC curve obtained from MS. Evolution of water vapor was identified by the simultaneous detection of sets of $m/z = 18$ (H$_2$O$^+$) and 17 (OH$^+$) ions. In the present work, the abundance ratio of [OH$^+$]/[H$_2$O$^+$] was approximately 30.2% which is higher than that (21.2%) of reference spectra reported in the NIST database [21]. The difference should be attributed to the instrumental difference. The estimated mass loss 24.53% agreed with the theoretical value corresponding to the thermal dehydration of the six water molecules (24.13%). The amorphous intermediate was indicated by XRD analysis of the specimen which was quenched from the TG–DTA apparatus at $150°C$ (above the dehydration). A sharp exothermic DTA phenomenon was observed immediately after the dehydration at $194°C$. Only formation of copper acetate, Cu(CH$_3$CO$_2$)$_2$, was a little con-

Fig. 1. TG, DTG and DTA curves for thermal decomposition of CaCu(CH$_3$CO$_2$)$_4$·6H$_2$O.

firmed by the XRD analysis in which the specimen was quenched from the TG–DTA apparatus at 225°C. After the exothermic phenomenon both of $Cu(CH_3CO_2)_2$ and $Ca(CH_3CO_2)_2$ might be formed independently. We leave a detailed discussion about them for another opportunity and will be made further experiments in the near future.

The second decomposition stage was observed at around 300°C, and the TG, DTG , DTA and TIC curves (Fig. 3) that it proceeds in four endothermic mass loss steps with a total mass loss of 30.15%. The
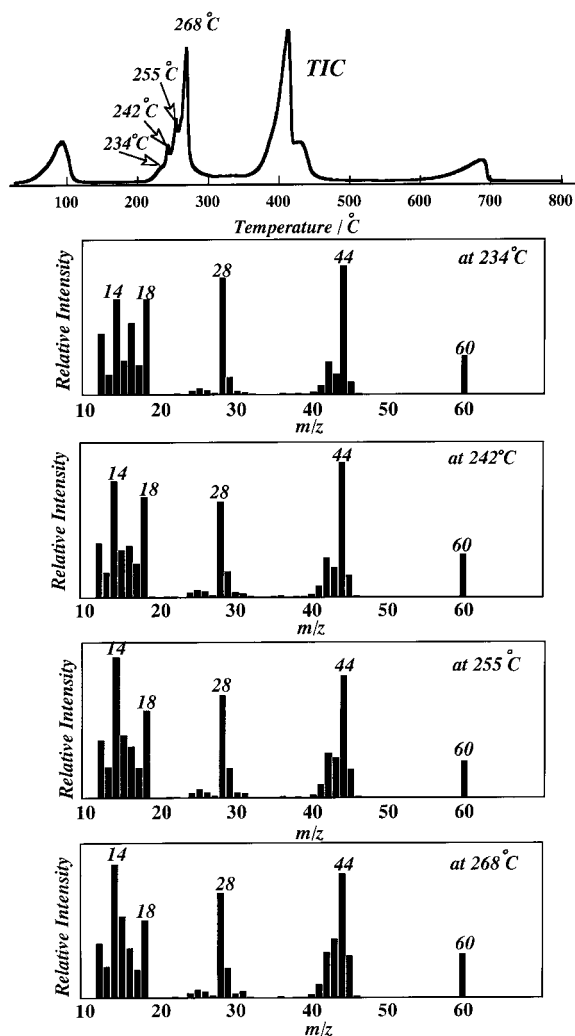

Fig. 3. TIC curve and mass spectra observed at 243°C, 242°C, 255°C and 268°C, respectively.

mass spectra observed at the TIC peak temperatures (234°C, 242°C, 255°C and 268°C) seem to be similar to each other. The components of the evolved gases were identified as a mixture of carbon monoxide ($m/z = 12$, 16 and 28) [22], carbon dioxide ($m/z = 16$, 28 and 44) [23], acetic acid ($m/z = 15$, 43, 45 and 60) [24] and water vapor ($m/z = 17$ and 18). We could not assign the other evolution components with the small amount of the additional fragment ions. These facts suggest that every step consists of similar succeeding decomposition reactions.

In the third decomposition stage proceeding at around 480°C, the TG and DTG curves indicate that the apparent two consecutive decompositions occurred with endothermic mass losses, 11.46%. The mass spectra for the third stage are shown in Fig. 4. The fragment ion patterns for both the peak temperatures (412°C and 430°C) in the TIC curve were also similar to each other, and the original source could be identified as acetone ($m/z = 15$, 43 and 58) [25].

The final decomposition stage at around 700°C was an endothermic mass loss of 10.22%. The smoothness of TG–DTA curves suggested that the stage takes place without any intermediates. The TIC curve for the stage shows a peak at 686°C (Fig. 5). Simultaneous evolution of carbon dioxide and carbon monoxide was recognized from the mass spectrum. Formation of carbon monoxide is assumed because the intensity of molecular ions ($m/z = 28$) was higher than expected from fragmentation of carbon dioxide.

In order to determine the decomposition mechanism, the evolved components identified should be correlated to the mass losses during each decomposition stage. The first endothermic mass loss corresponds to the dehydration:

$$CaCu(CH_3CO_2)_4 \cdot 6H_2O$$
$$\rightarrow CaCu(CH_3CO_2)_4 + 6H_2O \quad (1)$$
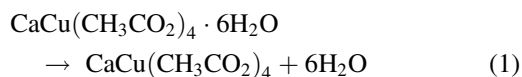
However, the reaction mechanism of the second stage cannot explain directly from the observed evolution components because the several decompositions occur continuously. Contrary to the prior expectations, it is difficult to unambiguously characterize these complicate reaction mechanisms by use of the simple TG–MS technique.

From this point of view, if the temperature of sample is controlled with the increasing of decom-
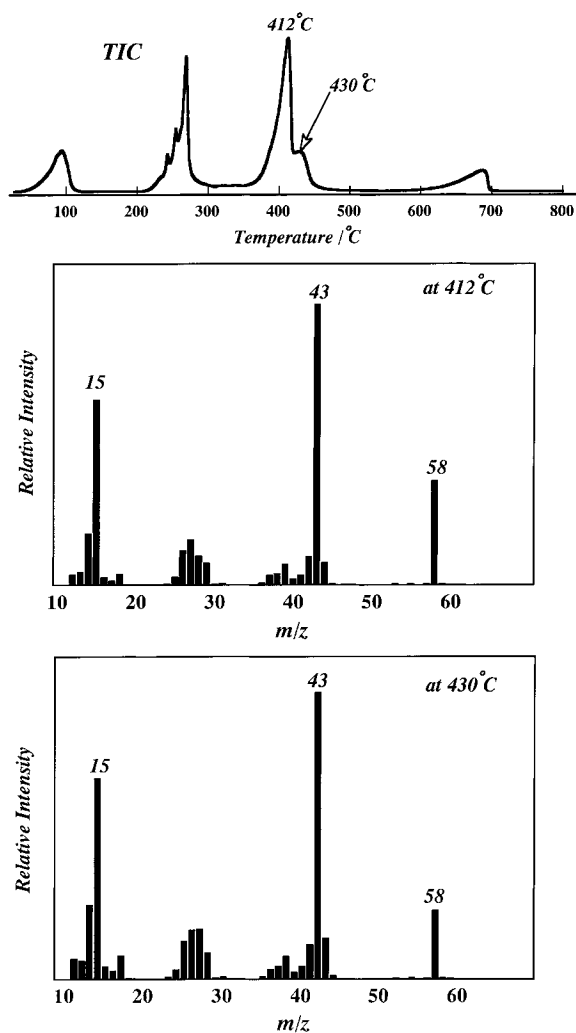
Fig. 4. TIC curve and mass spectrum observed at TIC peaks of 412°C and 430°C.

Fig. 5. Mass spectra observed at 686°C in TIC curve.

Fig. 6. Comparison of mass loss curves for decomposition using conventional TG of $3°C\,min^{-1}$ with that using CRTG of $0.06\%\,min^{-1}$.

position rate, it may enable to prevent the additional reaction and to observe independently the each reaction step. To satisfy the requirements, we need to incorporate CRTG technique in which all reaction stages are treated on the basis of equilibrium concept.

Fig. 6 illustrates the mass loss curves of $CaCu(CH_3CO_2)_4 \cdot 6H_2O$ depicted as a function of temperature using conventional TG and CRTG. The most important part of CRTG is that the heating rate is decreasing with increasing of the decomposition rate, so that the parallel additional reaction can be prevented effectively. It was noteworthy that the significant
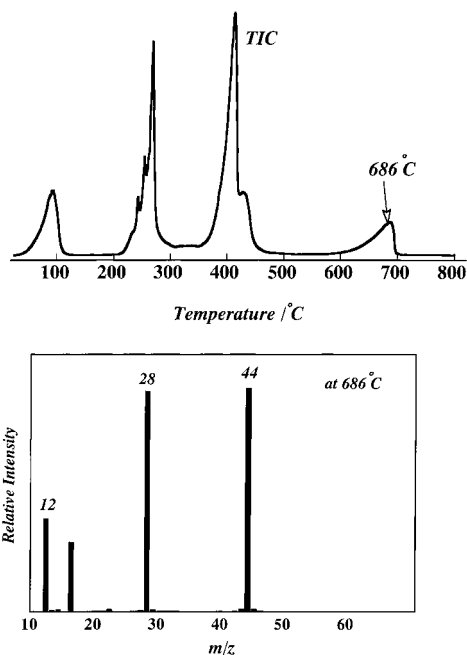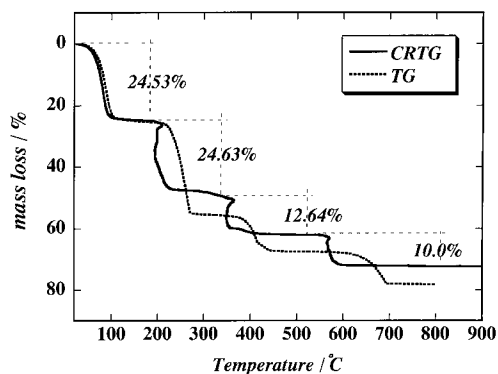
decomposition steps of CRTG were effectively shifted to lower temperature sides and the decomposition temperature ranges of CRTG became narrower than those of the conventional TG. The second point was that the large differences of the total mass loss percentages were observed between both the experiments. These results suggested that each decomposition proceeds through the different decomposition mechanism.
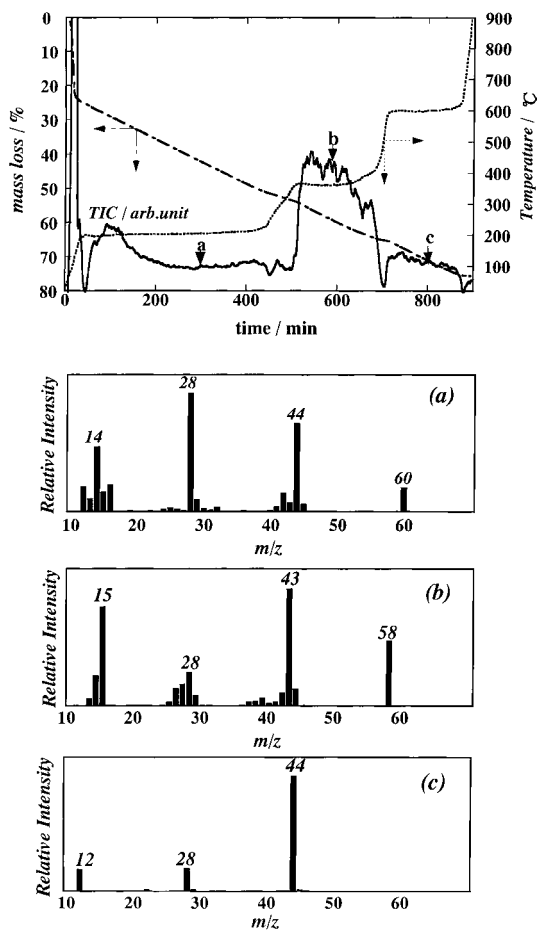
Fig. 8. XRD profile for intermediate quenched at 275°C in CRTG experiment. Cu_2O and $Ca(CH_3CO)_2 \cdot 0.5H_2O$ were identified as residual products. Key: (*), Cu_2O; (▼), $Ca(CH_3CO)_2 \cdot 0.5H_2O$; (▽).

Fig. 7. Overall mass loss, temperature and TIC curves for simultaneous CRTG–MS at 0.06% min^{-1}, and mass spectra obtained at (a) 202°C, (b) 361°C, and (c) 603°C, respectively.

Fig. 7 shows the results of CRTG–MS, and Fig. 7a illustrates the mass spectrums of the evolved gases of the middle region (202°C) during the second decomposition stage. The mass loss values agreed with those expected from these components. The gas components evolved simultaneously were identified as carbon monoxide, carbon dioxide, acetic acid and CH_2 ($m/z = 14$). The evolution of CH_2 seemed to exist independently since its m/z 14 ion could not be followed from the fragmentation of the simultaneously evolved components.

In order to understand the decomposition mechanism, it is important to identify the intermediates formed in the solid phase. Fig. 8 shows the XRD
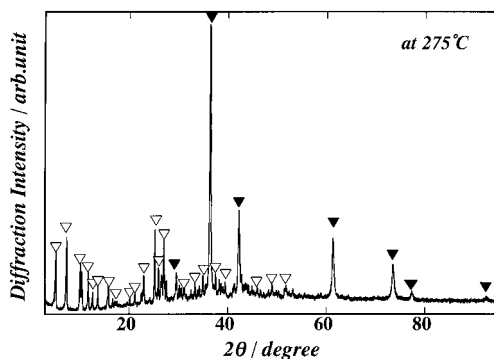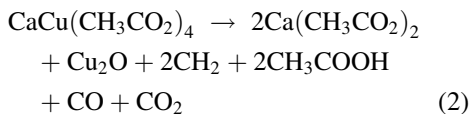
diagram for the intermediate quenched immediately after the second decomposition stage on CRTG (275°C). The intermediate was identified as a mixture of cuprous oxide (Cu_2O) and calcium acetate hemihydrate ($Ca(CH_3CO_2)_2 \cdot 0.5H_2O$) from its XRD pattern. Presumably, the anhydrous product, $Ca(CH_3CO_2)_2$, formed in the decomposition with CRTG seemed to be immediately hydrated to the hemihydrate with the atmospheric water vapor. This hypothesis was supported by the dehydration which was clearly observed at around 150°C in the re-heating TG–MS experiment of the quenched sample.

The second endothermic mass loss in CRTG corresponds to the following decomposition reaction:

$$
\begin{aligned}
CaCu(CH_3CO_2)_4 &\rightarrow 2Ca(CH_3CO_2)_2 \\
&+ Cu_2O + 2CH_2 + 2CH_3COOH \\
&+ CO + CO_2
\end{aligned} \tag{2}
$$

The mass loss (24.63%) agreed very closely with the theoretical value (24.58%). Fig. 7b shows the mass spectrum obtained at 361°C. Both, the spectrum and the mass loss of 12.64% corresponded to the evolution of acetone (theoretical amount 12.97%) as described by

$$
Ca(CH_3COO)_2 \rightarrow CaCO_3 + CH_3COCH_3 \tag{3}
$$

Fig. 7c shows the mass spectra observed at 603°C for the mass loss of 10.0%, to estimate the final decomposition stage. Only evolution of carbon dioxide was noted by the detection of $m/z = 12$, 28 and 44
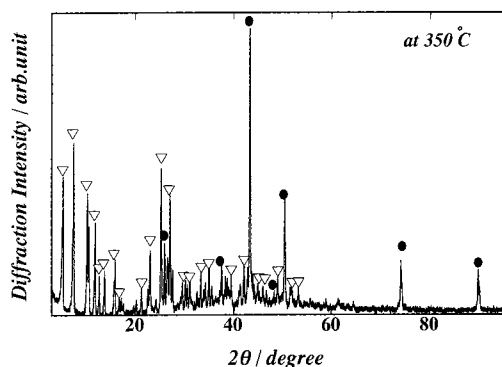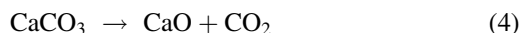
Fig. 9. XRD profile for intermediate obtained at 350°C in conventional TG experiment. Cu and $Ca(CH_3CO)_2 \cdot 0.5H_2O$ were identified as residual products. Key: (*), Cu; (●), $Ca(CH_3CO)_2 \cdot 0.5H_2O$; (▽).

ions with the characteristic intensity. The mass loss agreed with the theoretical value (9.83%) for the release of CO_2 according to

$$CaCO_3 \rightarrow CaO + CO_2 \qquad (4)$$

This result suggests that CRTG gives us more reliable and detailed information of the decomposition mechanism than the conventional linear heating thermal analysis. Because the evolution rate of gaseous products is roughly controlled by use of CRTG, the rate of reaction can also be controlled. Such advantage of CRTG seems to give an useful clue to explain the present decomposition.

The difference of the mass loss profiles on the CRTG and TG curves suggested that the decomposition processes in both the thermogravimetries were different to each other. In order to confirm the different decomposition processes in CRTG and TG, we would like to deal with the second stage, where the difference of the mass loss was observed remarkably in both thermogravimetries. Fig. 9 shows the results of XRD for the intermediate products quenched immediately after the second decomposition stage of the conventional TG (350°C). The quenched product was identified as a mixture of copper metal and calcium acetate hemihydrate, which was different from that of CRTG (Fig. 8). The critical difference was that copper was formed in the conventional TG but cuprous oxide was formed in the CRTG.

In order to discuss these differences, the ratio of $m/z = 28$ (CO)–$m/z = 44$ (CO_2) ions obtained from the conventional TG (Fig. 3) was compared with that from the CRTG (Fig. 7a). The CO_2 evolved under the TG was obviously larger than that under the CRTG. These findings seem to be ascribable as follows. Since many decomposition steps occur continuously under the conventional TG, CO and Cu_2O formed in the step (2) seems to be able to react

$$Cu_2O + CO \rightarrow Cu + CO_2 \qquad (2a)$$
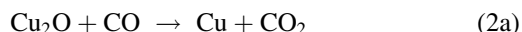
Both the lowered decomposition temperature and the lower partial pressure of potentially reducing species of CO and CH_2 were realized under the conditions of CRTG, so that reaction (2a) does not occur. This is the reason why Cu metal was formed under the conditions of the conventional TG whereas Cu_2O was formed under the conditions of CRTG. These findings are also consistent with the result that the mass loss of the second stage for the conventional TG is larger than that for the CRTG.

4. Conclusions

The TG–MS using conventional thermal analysis showed that the thermal decomposition of calcium copper acetate hexahydrate in helium atmosphere consisted of apparently four steps. Since the several successive reactions took place concurrently and the additional reactions progressed especially in higher temperature ranges, it was virtually difficult to clarify the decomposition mechanisms by the conventional TG. If the reaction temperature and the partial pressure of self-generated components around the sample are controlled by CRTG, the formation of the new intermediate products can be expected by selecting the appropriate rate of reaction. This finding suggested that the combination system of CRTG and the simultaneous EGA using MS is effective to clarify the complicated decomposition. The reaction mechanism (reactions (1)–(4)) was formulated satisfactorily for this decomposition by use of the combined system of CRTG–MS. In the conventional TG, step (2) is followed by reaction (2a).

Although the result of the present study is yet incomplete, it has shown the usefulness of the combination analysis of CRTG and MS to study the mechanism of the complicated decompositions. The simultaneous measurement of CRTG and MS was a

useful method to study the present decomposition mechanism.

References

[1] R. Baker, J. Hudec, Chemical Comunications (1967)890.

[2] E.A. Klop, A.J.M. Duisenberg, A.L. Spek, Acta Cryst. 39 (1983) 1342.

[3] K. Minagawa, Y. Masuda, W. Morita, Z. Zhong, P.K. Gallagher, Y. Masuda, The 32nd Japanese Conference on Calorimetry and Thermal Analysis, 1996, p. 22.

[4] S. Shirotoshi, M. Minagawa, P.K. Gallagher, Z. Zhong, The 31st Japanese Conference on Calorimetry and Thermal Analysis, 1995, p. 158.

[5] T. Arii, Y. Kobayashi, A. Kishi, Thermochim. Acta 325 (1999) 151.

[6] T. Arii, A. Kishi, Thermochim. Acta 325 (1999) 157.

[7] E.K. Gibson Jr., S.M. Jonson, Thermochim. Acta 4 (1972) 49.

[8] J. Chiu, A.J. Battie, Thermochim. Acta 50 (1981) 49.

[9] T. Arii, T. Senda, N. Fujii, Thermochim. Acta 267 (1995) 209.

[10] M. Mittleman, Thermochim. Acta 166 (1990) 301.

[11] R. Kinoshita, Y. Teramoto, T. Nakano, H. Yoshida, J. Thermal Anal. 38 (1992) 1891.

[12] J. Rouquerol, J. Thermal Anal. 2 (1970) 123.

[13] J. Rouquerol, Thermochim. Acta 144 (1989) 209.

[14] F. Paulik, J. Paulik, Thermochim. Acta 100 (1986) 23.

[15] J.M. Criado, F.J. Gotor, A. Ortega, C. Real, Thermochim. Acta 199 (1992) 235.

[16] J.M. Criado, F.J. Gotor, C. Real, F. Jimenez, S. Ramos, J. Del Cerro, Ferroelectrics 115 (1991) 43.

[17] J. Rouquerol, Thermochim. Acta 300 (1997) 247.

[18] T. Arii, N. Fujii, J. Anal. Appl. Pyrolysis 39 (1997) 129.

[19] T. Arii, H. Nakagawa, Y. Ichihara, N. Fujii, Thermochim. Acta 319 (1998) 139.

[20] T. Arii, J. Mass Spectrom. Soc. Jpn. 46 (1998) 374.

[21] Entry No. 4, NIST 107 (H_2O).

[22] Entry No. 8, NIST 107 (CO).

[23] Entry No. 36, NIST 107 (CO_2).

[24] Entry No. 103, NIST 107 (Acetic acid).

[25] Entry No. 125, NIST 107 (Acetone).